Published OnlineFirst August 10, 2018; DOI: 10.1158/1535-7163.MCT-18-0174

Companion Diagnostic, Pharmacogenomic, and Cancer Biomarkers

Molecular Cancer Therapeutics

Noninvasive Detection of ctDNA Reveals Intratumor Heterogeneity and Is Associated with Tumor Burden in Gastrointestinal Stromal Tumor

Heidi M. Namløs[1], Kjetil Boye[1,2], Skyler J. Mishkin[3], Tale Barøy[1], Susanne Lorenz[4], Bodil Bjerkehagen[5], Eva W. Stratford[1], Else Munthe[1], Brian A. Kudlow[3], Ola Myklebost[1,6], and Leonardo A. Meza-Zepeda[1,4,5]

Abstract

Molecular analysis of circulating tumor DNA (ctDNA) has a large potential for clinical application by capturing tumor-specific aberrations through noninvasive sampling. In gastrointestinal stromal tumor (GIST), analysis of *KIT* and *PDGFRA* mutations is important for therapeutic decisions, but the invasiveness of traditional biopsies limits the possibilities for repeated sampling. Using targeted next-generation sequencing, we have analyzed circulating cell-free DNA from 50 GIST patients. Tumor-specific mutations were detected in 16 of 44 plasma samples (36%) from treatment-naïve patients and in three of six (50%) patients treated with tyrosine kinase inhibitors. A significant association between detection of ctDNA and the modified National Institutes of Health risk classification was found. All patients with metastatic disease had detectable ctDNA, and tumor burden was the most important detection determinant. Median tumor size was 13.4 cm for patients with detectable mutation in plasma compared with 4.4 cm in patients without detectable mutation ($P = 0.006$). ctDNA analysis of a patient with disease progression on imatinib revealed that multiple resistance mutations were synchronously present, and detailed analysis of tumor tissue showed that these were spatially distributed in the primary tumor. Plasma samples taken throughout the course of treatment demonstrated that clonal evolution can be monitored over time. In conclusion, we have shown that detection of GIST-specific mutations in plasma is particularly feasible for patients with high tumor burden. In such cases, we have demonstrated that mutational analysis by use of liquid biopsies can capture the molecular heterogeneity of the whole tumor, and may guide treatment decisions during progression. *Mol Cancer Ther; 17(11); 2473–80. ©2018 AACR.*

Introduction

Gastrointestinal stromal tumor (GIST) is the most frequent mesenchymal tumor in the gastrointestinal tract. The key molecular drivers of GIST are mutations in *KIT* (80%) or *PDGFRA* (15%; ref. 1), and the majority of GISTs with such mutations are sensitive to tyrosine kinase inhibitors (TKI; ref. 2). Imatinib is the preferred first-line treatment for most patients with inoperable or metastatic disease (3). The likelihood of tumor response depends on the mutational profile, with exon 11 mutated *KIT* being the most sensitive to imatinib. The majority of patients with metastatic GIST eventually develop imatinib resistance, most often as a result of secondary mutations in the same allele as the original mutation (4). The currently approved second- and third-line treatments are sunitinib and regorafenib, respectively. Their antitumor effects are associated with the type of *KIT* or *PDGFRA* resistance mutation present (5, 6). Still, because of considerable intra- and intertumor heterogeneity, the clinical utility of identifying resistance mutations in biopsies from metastatic lesions is limited (7).

Small amounts of fragmented circulating cell-free DNA (cfDNA) of tumor origin (ctDNA) are continuously released to the blood stream. The main release process is through apoptosis, with additional contribution from necrosis or active secretion (8, 9). Several studies have demonstrated a high concordance between mutational profiles of candidate genes in matched tumor and plasma DNA samples (10–12). Detection of ctDNA in other cancers has been correlated with clinical and pathologic risk factors like tumor volume, lymph node involvement, and necrosis, associating detection of ctDNA with a more aggressive disease (13).

GIST has a well-known spectrum of actionable kinase mutations giving a strong relationship with tumor response to TKIs. This, combined with the need for analyses that reflect the total mutational landscape in each patient at each time point, provides a strong rationale for obtaining tumor material for molecular analyses through noninvasive liquid biopsies. Such blood plasma biopsies have a potential application in diagnosis, prognosis,

[1]Department of Tumour Biology, Institute for Cancer Research, Oslo University Hospital, Oslo, Norway. [2]Department of Oncology, Oslo University Hospital, Oslo, Norway. [3]Archer DX Inc., Boulder, Colorado. [4]Genomics Core Facility, Department of Core Facilities, Oslo University Hospital, Oslo, Norway. [5]Department of Pathology, Oslo University Hospital, Oslo, Norway. [6]Department of Clinical Science, University of Bergen, Bergen, Norway.

Note: Supplementary data for this article are available at Molecular Cancer Therapeutics Online (http://mct.aacrjournals.org/).

H.M. Namløs and K. Boye contributed equally to the article.

Corresponding Author: Leonardo A. Meza-Zepeda, Institute for Cancer Research, Oslo University Hospital, The Norwegian Radium Hospital, Ullernchausseen 70, Oslo 0379, Norway. Phone: 47-99035706; E-mail: Leonardo.Meza-Zepeda@rr-research.no

doi: 10.1158/1535-7163.MCT-18-0174

Published OnlineFirst August 10, 2018; DOI: 10.1158/1535-7163.MCT-18-0174

monitoring of disease progression, and evolution and prediction of therapy response (13). Only a few studies of ctDNA in GIST have been reported; mutant ctDNA has been detected in plasma from patients with GIST, and the amount was correlated with the disease course (14) and tumor size (15). Secondary *KIT* mutations that confer treatment resistance have also been identified from liquid biopsies (16).

In this study, targeted next-generation sequencing (NGS) was performed to detect *KIT* and *PDGFRA* mutations with high sensitivity in ctDNA from patients with GIST. Detection of ctDNA was significantly associated with high tumor burden, and clinical utility was demonstrated by capturing of molecular tumor heterogeneity and disease monitoring by liquid biopsies.

Material and Methods

Patient cohort

From October 2014, all patients diagnosed with GIST at Oslo University Hospital have been included in the NoSarC study, in which blood, plasma, serum, and fresh frozen tumor tissue are collected from all patients diagnosed with sarcoma in Norway. For the present study, we selected patients with GIST included between October 2014 and September 2016.

The study was approved by the Regional Ethics Committee of South East Norway (#S-06133a), and written informed consent was obtained from all patients. The study was performed in accordance with the Declaration of Helsinki.

Risk classification was performed according to the modified NIH criteria (17). Tumor size was measured on the surgical specimen, except for patients who received preoperative imatinib in whom CT scan before treatment start was used. Mitoses were counted in all specimens, except biopsies and specimens subjected to neoadjuvant therapy. Mutation analysis in routine practice was performed as previously described (18).

Extraction and quantification of DNA

Blood was collected in Cell-Free DNA BCT tubes (Streck), and plasma and normal white blood cells were processed as previously described (19) and stored at −80°C. cfDNA, representing both normal and tumor DNA, was isolated from 2 to 4 mL (average 2.2 mL) plasma using QIAamp Circulating Nucleic Acid Kit (Qiagen) and stored at −20°C. Normal genomic DNA from white blood cells was isolated using QIAamp DNA Mlood Mini Kit (Qiagen).

Tumor material was fresh frozen at −80°C immediately after surgery. Two tissue sections were stained with hematoxylin and eosin, and the presence of representative tumor material (>60% tumor cells) was verified by a sarcoma pathologist. Genomic DNA was isolated using the Allprep DNA/RNA Kit (Qiagen) and the truXTRAC FFPE DNA Kit (Covaris Inc.) from fresh frozen tumor and formalin-fixed paraffin-embedded (FFPE) tissue (20), respectively.

Genomic DNA was quality controlled using Nanodrop 2000 (Thermo Fisher Scientific) and genomic DNA and cfDNA were quantified using a Qubit fluorometer from Invitrogen (Thermo Fisher Scientific).

Library construction and sequencing using Archer targeted panel

Sequencing libraries were made from 15 ng of cfDNA for screening of the GIST cohort and 40 ng cfDNA for the case patient. The libraries were made following the Archer Reveal ctDNA 28 Kit for Illumina (ArcherDX Inc.), providing targeted exon sequencing of 28 cancer-related genes. For the case study, sequencing libraries were additionally made from 100 ng of DNA from FFPE and 50 ng from fresh frozen tumor and normal gDNA using the Archer VariantPlex Assay system (ArcherDX, Inc.). For the case study and some of the GIST cfDNA samples in the screening, the Archer Reveal ctDNA gene enrichment panel was customized to include exon 14 of *KIT*. The libraries were pooled and paired-end sequenced (2 × 150 bp) with 20% PhiX using Illumina's sequencing by synthesis technology (SBS) on a NextSeq500 instrument (Illumina Inc.).

Bioinformatics analysis of cfDNA data from Archer targeted panel

The sequencing data were processed using Archer Analysis (v5.1) pipeline. Each read associated with a unique Molecular Barcode (MBC) was used to create a single consensus read, using the base call quality scores from primary analysis. The germline and somatic mutation detection pipeline mapped reads to the hg19 (GRCh37) reference genome using Bowtie 2 (21) and postprocessed the alignments. Variant calling was performed using FreeBayes (22) and LoFreq (23).

The default ctDNA with outlier filter in Archer Analysis was applied to the cfDNA data, keeping variants with alternate observations (AO) $\geq$ 5, unique alternate observations (UAO) $\geq$ 3, exome aggregation consortium (ExAC) global population allele frequency (AF) $\leq$ 0.05, variants that have a consequence, variants called by Vision variant caller and with an AF outlier *P*-value $\leq$0.01. The AF outlier *P*-value describes the probability of this mutation to be background noise, as estimated across all samples processed in the same analysis run.

Manual inspection of BAM files was performed to identify mutations in *KIT* or *PDGFRA* that were known from the tumor, but not retained in the analysis of cfDNA. Patients with *KIT* duplications were not included in the study because preliminary data showed difficulties in the detection of these types of aberrations. Analysis of ctDNA data was conducted in a blinded fashion with respect to the clinical information of individual patients.

Library construction and sequencing of cfDNA using Swift targeted panel

The findings from the case study were verified using The Accel-Amplicon 56G Oncology Panel from Swift Biosciences (Swift Biosciences). In this panel, 56 cancer genes were represented, including *KIT* and *PDGFRA*. Fifteen nanograms of cfDNA was used as input, and multiplex PCR and indexing were done to generate dual indexed libraries. The libraries were pooled with 2% PhiX and sequenced pair-end (2 × 150 bp) using SBS chemistry on a MiSeq v3 instrument (Illumina Inc.). Reads preprocessing with adapter trimming, mapping, alignment, quality assessment, and variant calling were performed using MiSeq Reporter. Manual inspection of BAM files was performed, identifying additional somatic mutations in *KIT*.

Targeted exome sequencing of DNA

Sequencing libraries were prepared from 1 μg DNA from the GIST tumor and normal samples following the SureSelectXT All Exon V5 protocol (Agilent Technologies). The libraries were sequenced paired-end (2 × 100 bp) on a HiSeq2500 (Illumina, Inc.) using TruSeq SBS v3 chemistry. Real-time analysis and

Published OnlineFirst August 10, 2018; DOI: 10.1158/1535-7163.MCT-18-0174

base calling were conducted by Illumina's software packages HSC2.0.2/RTA1.17.21.3. Raw reads were processed using the Illumina CASAVA (v. 1.8.2) to demultiplex data and filter out the low-quality reads. The mapping, alignment, quality assessment, and somatic variant calling were performed as previously described (19).

Because of Norwegian legal regulations, we are not able to deposit our dataset in a public repository. We will provide access to the data upon request.

Statistical analysis

Relationships between ctDNA detection and the categorical variables gender, primary tumor localization, and NIH risk classification were analyzed using Pearson's chi-square test. Differences in age, tumor size, and mitotic count between patients with and without detectable ctDNA were analyzed using independent samples Mann–Whitney *U* test. Data analysis was performed using SPSS version 21.0 (SPSS Inc.). *P*-values < 0.05 were considered statistically significant.

Results

Patient characteristics

From October 2014 to September 2016, 50 patients diagnosed with localized or metastatic GIST were included in the study. These included 44 newly diagnosed patients, where blood samples were collected before treatment. In addition, we analyzed samples from six patients undergoing TKI treatment at the time of plasma sampling. Routine molecular diagnostics were performed on all 50 tumors; a *KIT* mutation was detected in 41 of the tumors, and the remaining nine tumors had a *PDGFRA* mutation (Supplementary Table S1).

Demographic, clinical, and histopathologic characteristics for the 44 treatment naïve patients are summarized in Table 1. These included 25 males (57%) and 19 females (43%), with a median age of 65 years (range 33–93). Thirty-four patients (77%) had localized disease and 10 patients (23%) had metastatic disease at time of inclusion.

Table 1. Demographic, clinical, and histopathologic characteristics of the 44 treatment-naïve patients

Age at inclusion	
Median (range)	65 (33–93)
Gender	
Female	19 (43)
Male	25 (57)
Primary tumor localization	
Stomach	36 (82)
Small intestine	6 (14)
Oesophagus	2 (5)
Median tumor size (range)[a]	5.1 (2.5–20.0)
Median mitotic count (range)[a]	3 (0–24)
Modified NIH risk classification	
Low risk	12 (27)
Intermediate risk	7 (16)
High risk	15 (34)
Metastatic	10 (23)
Mutation analysis	
KIT exon 11	33 (75)
KIT exon 13	1 (2)
KIT exon 17	1 (2)
PDGFRA exon 12	1 (2)
PDGFRA exon 18	8 (18)

Number of patients and percentage (in parentheses) is shown unless otherwise indicated.

[a]Data from patients with localized disease only.

Molecular profiling of treatment-naïve GIST using cfDNA

Blood samples of the 44 treatment naïve patients were drawn before surgery or start of systemic treatment. As all primary tumors had *KIT* ($n = 35$) or *PDGFRA* ($n = 9$) somatic mutations (Table 1), targeted exon panel sequencing was done to identify these mutations in the patients' plasma. Somatic mutations in *KIT* or *PDGFRA* in cfDNA, representing detected ctDNA, were found in 16 of 44 (36%) of the plasma samples (Fig. 1; Supplementary Table S1). Eleven of the mutations were identified directly using the Archer Analysis pipeline on the NGS data, and the remaining five mutations were identified by manual inspection of the BAM files.

A difference in the detection rate was seen dependent on type of mutation. Among the 21 patients having tumors with *KIT* indels, mutations were detected in 57% of the plasma samples. The median mutated allele frequency (AF) in cfDNA was 4.6% (range 0.07%–48.1%), corresponding to a median of 115 mutated genomes per milliliters of plasma (range 1–5,762). However, among the 14 patients having tumors with *KIT* single-nucleotide variants (SNV), mutations were only detected in 21% of the plasma samples with a median AF of 1.4% (range 1.1%–1.5 %) corresponding to a median of 75 mutated genomes per milliliters of plasma (range 53–77). For patients with a *PDGFRA* mutation, deletions were only detected in one of three plasma samples, whereas none of the six SNVs were detected in plasma. Furthermore, the highest fractions of ctDNA in cfDNA were mainly observed for patients having indels in exon 11 of *KIT* (Fig. 1; Supplementary Table S1). Except for one patient with a *TP53* mutation (Supplementary Table S1), no mutations in the other 26 genes of the Archer panel were detected in the plasma samples.

Detection of ctDNA is associated with clinical characteristics

Routine classification of GIST in Norway is performed using the modified NIH risk classification, which takes into account tumor size and mitotic count to stratify patients. A significant association between the NIH risk classification and detection of mutations was found. The somatic mutations were significantly more frequently detected in plasma from patients with higher risk classification or metastatic disease ($P < 0.001$; Fig. 2A). All 10 patients with metastatic disease had detectable mutated DNA in plasma, compared to 5 of 15 patients classified as high risk, 1 of 7 with intermediate risk and 0 of 12 with low risk GIST (Fig. 1). For patients with localized disease without detectable ctDNA, the median tumor size was 4.4 cm (range 2.5–16.6), compared with 13.4 cm (range 5.1–20.0) for patients with a detected mutation ($P = 0.006$; Fig. 2B). Among the 44 treatment naïve patients, mitotic count was only available for two of the six patients with detectable ctDNA and localized disease. The remaining tumors had received preoperative imatinib treatment, and counting of mitoses was thus not possible. No significant association with age, gender or primary tumor localization was found.

ctDNA detection in TKI-treated patients

Six patients who received TKI at the time of blood sampling were included as a second cohort. All patients had *KIT* mutations present in the tumor at time of diagnosis. For three of these patients, *KIT* mutations were also detected in plasma

Published OnlineFirst August 10, 2018; DOI: 10.1158/1535-7163.MCT-18-0174

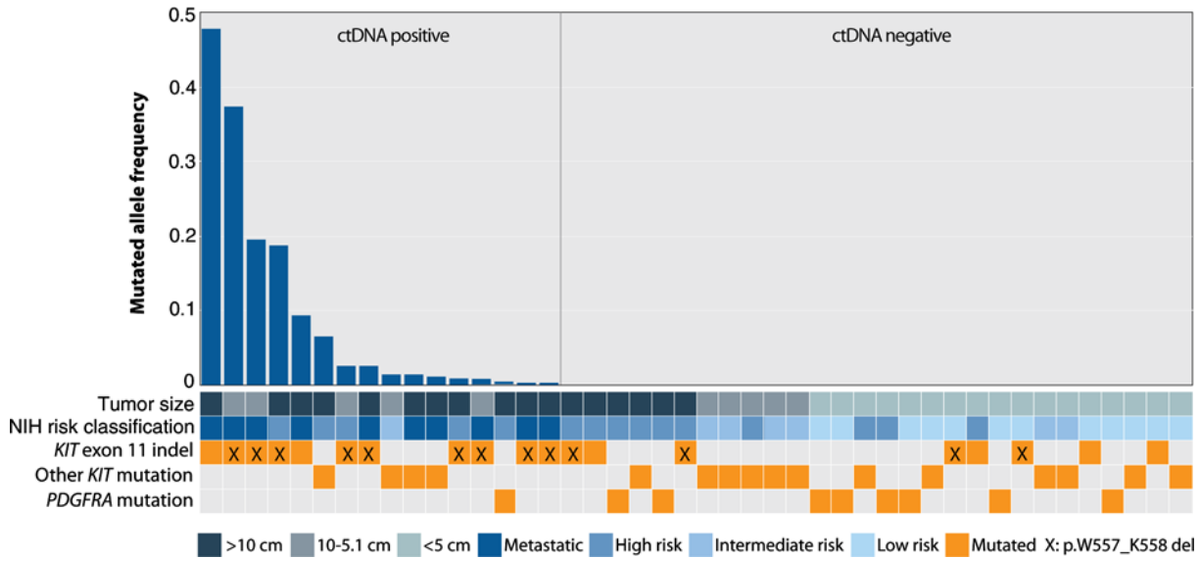

Figure 1.

Association between detection of mutated alleles in ctDNA, tumor size, NIH risk criteria, and mutation type in treatment-naïve GIST. The 44 newly diagnosed, treatment naïve patients were sorted based on mutated *KIT* or *PDGFRA* allele frequency for those with detected ctDNA in plasma (ctDNA positive) and sorted on tumor size for the remaining patients (ctDNA negative). The status for the variables tumor size, NIH risk classification, and mutation type are given below the graph.

(Supplementary Table S1). One patient underwent surgery for a rapidly progressing peritoneal metastasis after 3 years of imatinib treatment, and both the primary *KIT* exon 11 mutation and a secondary exon 13 mutation were detected both in plasma and in the surgical specimen. The second patient had detectable ctDNA after 9 months of imatinib treatment for a locally advanced gastric GIST with radiologic response, and 9 months later developed metastatic disease. For the third patient, both the primary and several secondary *KIT* mutations were detected upon disease progression after 8 months treatment with imatinib (see case below). In the remaining three patients, ctDNA was not detectable; the first patient had locally advanced gastric GIST and had received imatinib for 1 month with a good radiologic response, the second patient had received imatinib for 13 years for metastatic GIST and underwent surgery for a 2.8 cm solitary peritoneal metastasis, and the third patient had received sunitinib for 45 months and was operated for a symptomatic small intestinal primary tumor. Thus, detection of ctDNA in patients undergoing TKI treatment can be related to the disease development.

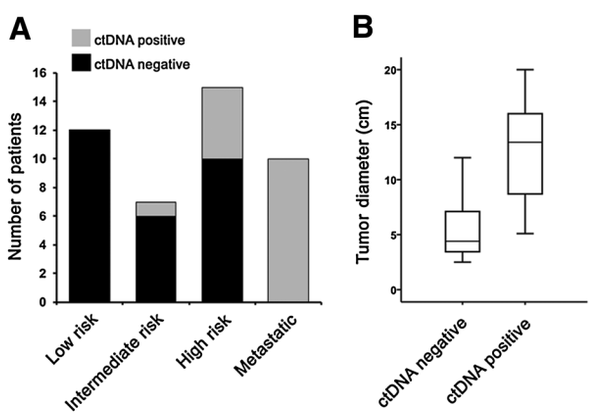

Figure 2.

Associations between ctDNA detection and tumor characteristics. **A,** Detection of somatic mutations (ctDNA positive or negative) in plasma across NIH risk classification categories, analyzed using Pearson chi-square test ($P < 0.001$). **B,** Boxplots showing tumor size in patients with or without detection of somatic mutations in plasma (ctDNA positive or negative). Boxes indicate the median, the 25th and 75th percentile, and whiskers represent maximum and minimum values. Outliers are censored. Analyzed using independent samples Mann–Whitney *U* test ($P = 0.006$).

ctDNA reveals intratumor heterogeneity

One of the patients included in the TKI treated cohort above was subject to a more comprehensive study. A 47-year-old male was referred to the Norwegian Radium hospital with a locally advanced 20 × 11 × 11 cm large gastric tumor, and percutaneous biopsy revealed a GIST with a *KIT* exon 11 p.W557_K558del mutation. He was considered primary inoperable and imatinib was started. After an initial treatment response, a CT scan 8 months after imatinib initiation showed progressive disease (Supplementary Fig. S1). No metastases were detected. A partial gastrectomy was performed. Routine mutational analysis and deep exome sequencing of the resected tumor identified the primary p.W557_K558del mutation, and a secondary resistance mutation in *KIT* exon 14 (p.T670I; Supplementary Tables S1 and S2).

At the time of surgery, both the primary p.W557_K558del mutation and the *KIT* exon 14 p.T670I mutation were identified in plasma using the Archer Reveal ctDNA panel. Notably, we also found three additional resistance mutations in exon 17 and 18, p.D816H, p.Y823D, and p.A829P, not previously identified in the surgical specimen (Fig. 3B; Supplementary Tables S1 and S2).

Published OnlineFirst August 10, 2018; DOI: 10.1158/1535-7163.MCT-18-0174

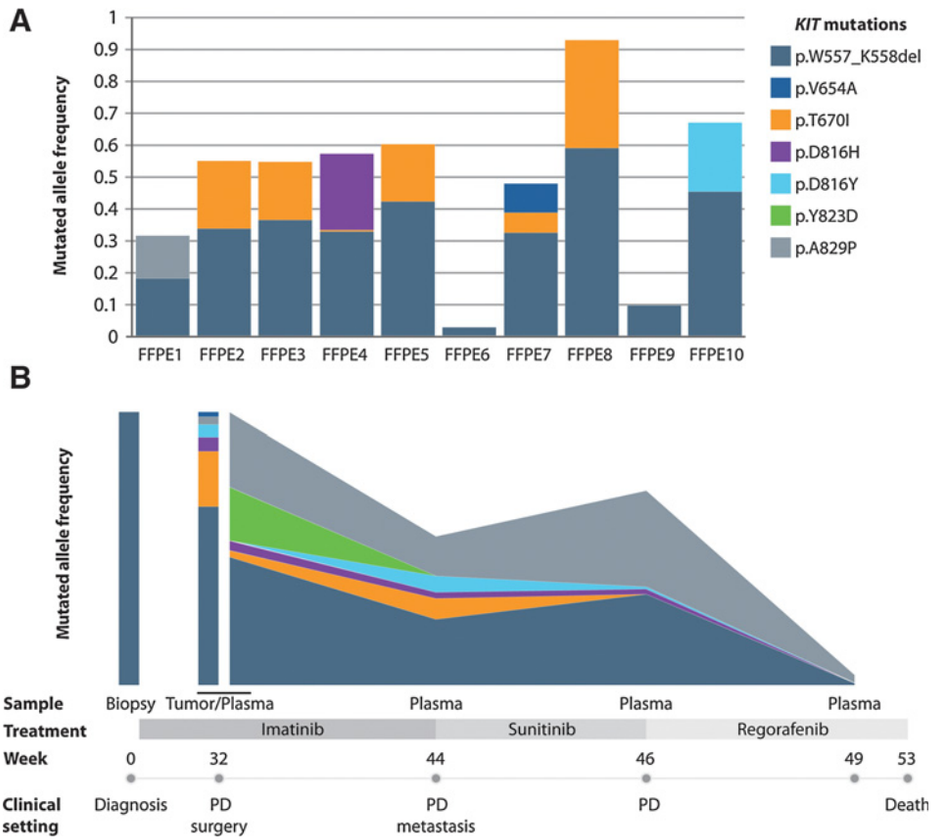

Figure 3.
Intratumor heterogeneity and clonal evolution of the tumor of a patient with GIST. **A,** *KIT* mutations identified in FFPE sections from different parts of the imatinib-treated tumor. Each bar represents data from one FFPE tumor specimen with the relative frequency of the indicated *KIT* primary and secondary mutations, based on Archer Reveal ctDNA sequencing. **B,** Evolution of tumor mutations during disease course of the patient. Shown allele frequencies of mutated *KIT* in fresh frozen biopsy at time of diagnosis, tumor at the time of surgery (average of the 10 FFPE specimens in **A**), and plasma before surgery at time of progressive disease (PD). Plasma samples were further collected at time of treatment change (to sunitinib or regorafenib). The amount (allele frequency) of each of the mutations is represented by the height of each curve, and then stacked on top of each other. The different mutations are identical colour coded in **A** and **B**.

All mutations detected in plasma were confirmed using the Accel-Amplicon 56G Oncology Panel from Swift Biosciences (Supplementary Table S2).

To validate the novel mutations identified in plasma, a comprehensive analysis of the tumor was performed. DNA extracted from the treatment naïve biopsy and from a surgical specimen was sequenced using the Archer Reveal ctDNA panel, and the surgical sample was also deep exome sequenced. No other *KIT* mutations than p.W557_K558del and p.T670I were found in either of these samples (Supplementary Table S2). During routine pathologic examination of the surgical specimen, 10 spatially separated samples from morphologically distinct parts of the tumor had been collected and formalin-fixed (Supplementary Fig. S2). Sequencing using the Archer Reveal ctDNA panel identified the primary *KIT* p.W557_K558del mutation in all 10 specimens, and the p.T670I resistance mutation in six samples. Two of the three other resistance mutations identified in plasma were also found in distinct regions of the tumor (p.D816H and p.A829P), whereas the p.Y823D mutation was not detected in the tumor tissue examined. Two tumor samples contained two different resistance mutations, and in two samples no resistance mutations were detected (Fig. 3A; Supplementary Table S3). A histologic evaluation was done on the FFPE tumor, grouping the sections into four categories based on the tumors relation to normal tissues; mucosa in stomach, serosa and fatty tissue. No association between the location of the tumor sections and the mutational pattern could be seen (Supplementary Fig. S2).

Monitoring clonal evolution throughout the treatment course using ctDNA

As a continuation of the patient story, repeated plasma samples from the case patient were collected during the subsequent treatment. Imatinib was continued after surgery, and 3 months postoperatively disseminated peritoneal metastases were evident (Supplementary Fig. S1). At this time point, four of the five *KIT* mutations present in plasma at time of surgery were detected, and also the p.D816Y mutation identified in the tumor tissue, but not in the initial plasma sample (Fig. 3B; Supplementary Table S2). Treatment with sunitinib was initiated. During treatment, the p.T670I mutation became undetectable and the p.D816H and p.D816Y mutations were significantly reduced, whereas the allele frequencies of the p.W557_K558del and p.A829P mutations increased (Fig. 3B; Supplementary Table S2). However, the peritoneal metastases rapidly progressed and the patient developed ascites fluid (Supplementary Fig. S1), leading to a switch to regorafenib after only 2 weeks of sunitinib therapy. After 3 weeks of regorafenib treatment, the patient's clinical condition was substantially better, and the only mutations detectable in plasma were p.W557_K558del and p.A829P. Seven weeks after commencement of regorafenib, the patient succumbed to progressive GIST.

Discussion

Acquisition of tumor material through liquid biopsies is currently being implemented in routine diagnostics and has a great potential for clinical utility in precision medicine. Using a targeted

Published OnlineFirst August 10, 2018; DOI: 10.1158/1535-7163.MCT-18-0174

NGS panel specifically designed for analysis of ctDNA, we have demonstrated that detection of GIST disease-causing mutations in plasma is significantly associated with the classification of tumors into risk groups. ctDNA was detected in all patients with metastatic disease. In localized GIST, mutations were only found in plasma from patients with large tumors. Thus, the greatest potential use of liquid biopsies seems to be for the more advanced cases where the clinical benefit of mutational monitoring may be most readily seen.

Two previous studies in GIST have also shown higher levels of ctDNA in larger tumors (14, 15). Maier and colleagues found that patients with measurable disease more often had detectable ctDNA, but a blood sample prior to start of treatment was only available for 9 of the 38 included patients (14). In a more recent study, the presence of mutant DNA in plasma was associated with a large tumor size, but not with mitotic count in patients with localized disease (15). Risk classification using Armed Forces Institute of Pathology (AFIP) criteria was, however, not associated with detectable ctDNA, but this analysis is limited by the fact that the vast majority of patients were classified as high risk. The lack of significant associations with mitotic count is also supported by our study. We were unable to detect ctDNA in two patients with tumors <5 cm and a high number of mitoses (19 and 24 per 50 HPF), suggesting that a high mitotic count itself is not associated with release of tumor DNA to the circulation. Our study, using a larger, more diverse cohort and a broader tumor size distribution than previous studies, clearly shows that ctDNA can be reliably detected in blood from GIST patients with a large tumor burden.

Patients with *KIT* exon 11 indels more often had detectable ctDNA than patients with other mutations. The reason for this observation might be that tumors with exon 11 indels, and in particular deletions involving codon 557 and 558, are larger and have a more malignant behavior (24–27). In our cohort, tumors with *KIT* exon 11 indels had a median tumor size of 10.9 cm compared to 5.1 for other tumors, and 16 of 20 patients with this genotype were classified as high risk or metastatic. Supporting this notion, the proportion of patients with detectable ctDNA is higher in patients with advanced disease for most tumor types (28).

Technological progress has brought about a number of highly sensitive methods for detection of ctDNA, such as amplification refractory mutation system (ARMS; ref. 29), BEAMing (beads, emulsion, amplification, and magnetics; ref. 30), digital droplet PCR (ddPCR; ref. 31), and whole genome NGS (32), reviewed in ref. 33. The use of small targeted NGS panels, covering a broad range of recurrent somatic variants, and the introduction of unique molecular barcodes with sophisticated bioinformatics analysis has facilitated the increased sensitivity required to analyze cfDNA. Liquid biopsies can be an excellent complementary source for genomic analysis, and with the input amounts of DNA and technique used in this project ctDNA can be readily detected in aggressive or larger tumors, but may not meet the sensitivity level required for monitoring minimal residual disease. In general, cancer patients show a high variability of cfDNA levels with fractions of ctDNA ranging from <1% to >90% dependent on tumor burden, stage, vascularity, cellular turnover, and response to therapy (reviewed in ref. 34). Thus, the sensitivity of the methods must be taken into account in study design, and robustness has to be evaluated in larger prospective studies.

The heterogeneity of resistance mutations between and within metastases is one of the main treatment challenges in patients with TKI-resistant GIST. The resistance mutations present in the patient tumor of the case study were diverse and were spatially distributed in the tumor. Our data demonstrate that the ctDNA is shed from multiple tumor subclones, and ctDNA can give improved representation of the intratumor heterogeneity and actionable alterations. Such substantial intratumor heterogeneity, as observed in this study, has not been previously described in GIST. It has been shown that imatinib-resistant disease frequently harbors up to two resistance mutations within a single tumor or metastasis, or up to five mutations in separate metastases from one patient (7, 35, 36), but not synchronously to such an extent within one primary tumor. Although it is not expected that all patients carry the same degree of heterogeneity, most TKI-resistant GISTs display a mutational heterogeneity that may be better captured by liquid biopsies than conventional analysis of tumor tissue.

The main therapeutic strategy in imatinib-resistant GIST during the past decade has been the introduction of multikinase inhibitors that target a broader spectrum of KIT resistance mutations. The resistance mutations detected after imatinib treatment clustered in two regions of the kinase domain: the ATP-binding pocket (encoded by exons 13 and 14) and the activation loop (encoded by exons 17 and 18), known to be essential for drug binding and kinase activation, respectively (37). During sunitinib treatment, we observed a reduction of ctDNA containing ATP binding domain mutations, whereas activation loop mutations seemed resistant to sunitinib. This is in line with previous clinical studies (38) and cell-based assays (39–41). Data from a phase II trial suggest that regorafenib, contrary to sunitinib, also show activity against mutations in the activation loop (42). During regorafenib treatment, the level of ctDNA decreased dramatically concurrently with clinical improvement. However, no radiologic response evaluation was performed, and the patient succumbed to the disease only 4 weeks later.

Our results suggest at least two potential applications that should be further investigated in GIST; monitoring of resistance mutations in imatinib-resistant disease and primary mutation analysis in cases with tumor tissue unsuitable for molecular analysis. In the latter situation, a biopsy of a locally advanced tumor planned for preoperative imatinib might return too little tumor tissue or DNA of too poor quality, but still contain sufficient material for diagnostic mutation detection. In the former scenario, the choice of systemic treatment after imatinib progression could be determined by the spectrum of resistance mutations in plasma. Liquid biopsies would be particularly useful to aid treatment choices of heterogeneous lesions. As an example, a patient with exclusively activation loop mutations, known to be less sensitive to sunitinib (38), could potentially benefit more from other TKIs like regorafenib. Even though the potential clinical utility is great, more comprehensive studies than those so far conducted are necessary before plasma mutation analysis of GIST can be implemented in a routine clinical setting. Several other cancer types, like lung cancer and colon, present recurrent mutations that could potentially be treated with a targeted approach. Monitoring of these patients using cfDNA is also highly relevant and feasible (10, 43, 44).

In conclusion, we have shown that liquid biopsies can be used as a source for mutational analysis of GISTs. A significant relationship was seen between detection of ctDNA and tumor risk classification, where tumor burden was found to be the most important determinant for ctDNA detection. We also

Published OnlineFirst August 10, 2018; DOI: 10.1158/1535-7163.MCT-18-0174

demonstrated that liquid biopsies better capture intratumor heterogeneity than conventional biopsies, and can be used to monitor clonal evolution throughout the treatment course of a GIST patient. Thus, our work strongly supports the rationale of using liquid biopsies as a source to obtain comprehensive mutational profiles of these heterogeneous tumors. Future studies should address the clinical utility of ctDNA in therapeutic decisions in imatinib-resistant metastatic GIST.

Disclosure of Potential Conflicts of Interest

B.A. Kudlow has ownership interest (including stock, patents, etc.) in ArcherDX. No potential conflicts of interest were disclosed by the other authors.

Authors' Contributions

Conception and design: H.M. Namløs, K. Boye, L.A. Meza-Zepeda
Development of methodology: H.M. Namløs, B.A. Kudlow, L.A. Meza-Zepeda
Acquisition of data (provided animals, acquired and managed patients, provided facilities, etc.): H.M. Namløs, K. Boye, S.J. Mishkin, T. Barøy, S. Lorenz, B. Bjerkehagen, E.W. Stratford, E. Munthe, O. Myklebost, L.A. Meza-Zepeda
Analysis and interpretation of data (e.g., statistical analysis, biostatistics, computational analysis): H.M. Namløs, K. Boye, S.J. Mishkin, L.A. Meza-Zepeda
Writing, review, and/or revision of the manuscript: H.M. Namløs, K. Boye, T. Barøy, S. Lorenz, B. Bjerkehagen, E.W. Stratford, E. Munthe, O. Myklebost, L.A. Meza-Zepeda
Administrative, technical, or material support (i.e., reporting or organizing data, constructing databases): K. Boye, O. Myklebost
Study supervision: L.A. Meza-Zepeda
Other (performed experiments): H.M. Namløs, T. Barøy

Acknowledgments

We would like to acknowledge Stine Næss for inclusion of patients in the NoSarC study, Heidi Anine K. Bjørhovde for processing of blood samples and tumor tissue, and Jinchang Sun at the Genomics Core Facility at Oslo University Hospital (oslo.genomics.no) for preparing sequencing libraries. The project was supported by funding from The Norwegian Cancer Society, grant no. PR-2007-0163 (to L.A. Meza-Zepeda) and 5790283 (to K. Boye), and the Research Council of Norway, grant no. 221580 (to O. Myklebost).

The costs of publication of this article were defrayed in part by the payment of page charges. This article must therefore be hereby marked *advertisement* in accordance with 18 U.S.C. Section 1734 solely to indicate this fact.

Received March 7, 2018; revised May 7, 2018; accepted August 3, 2018; published first August 10, 2018.

References

1. Patrikidou A, Domont J, Chabaud S, Ray-Coquard I, Coindre JM, Bui-Nguyen B, et al. Long-term outcome of molecular subgroups of GIST patients treated with standard-dose imatinib in the BFR14 trial of the French Sarcoma Group. Eur J Cancer 2016;52:173–80.
2. Demetri GD, von Mehren M, Blanke CD, Van den Abbeele AD, Eisenberg B, Roberts PJ, et al. Efficacy and safety of imatinib mesylate in advanced gastrointestinal stromal tumors. N Engl J Med 2002;347:472–80.
3. ESMO TESNWG. Gastrointestinal stromal tumours: ESMO Clinical Practice Guidelines for diagnosis, treatment and follow-up†. Ann Oncol 2014;25(suppl_3):iii21–6.
4. Fletcher J, Rege T, Liang CW, Raut C, Foley K, Flynn D, et al. 252 polyclonal resistance to kinase inhibition in GIST: mechanisms and therapeutic strategies. J Vasc Sci 2010;8:83.
5. Yeh CN, Chen MH, Chen YY, Yang CY, Yen CC, Tzen CY, et al. A phase II trial of regorafenib in patients with metastatic and/or a unresectable gastrointestinal stromal tumor harboring secondary mutations of exon 17. Oncotarget 2017;8:44121–30.
6. Reichardt P, Demetri GD, Gelderblom H, Rutkowski P, Im SA, Gupta S, et al. Correlation of KIT and PDGFRA mutational status with clinical benefit in patients with gastrointestinal stromal tumor treated with sunitinib in a worldwide treatment-use trial. BMC Cancer 2016;16:22.
7. Liegl B, Kepten I, Le C, Zhu M, Demetri GD, Heinrich MC, et al. Heterogeneity of kinase inhibitor resistance mechanisms in GIST. J Pathol 2008;216:64–74.
8. Jahr S, Hentze H, Englisch S, Hardt D, Fackelmayer FO, Hesch RD, et al. DNA fragments in the blood plasma of cancer patients: quantitations and evidence for their origin from apoptotic and necrotic cells. Cancer Res 2001;61:1659–65.
9. Stroun M, Lyautey J, Lederrey C, Olson-Sand A, Anker P. About the possible origin and mechanism of circulating DNA: apoptosis and active DNA release. Clin Chim Acta 2001;313:139–42.
10. Siravegna G, Mussolin B, Buscarino M, Corti G, Cassingena A, Crisafulli G, et al. Clonal evolution and resistance to EGFR blockade in the blood of colorectal cancer patients. Nat Med 2015;21:795–801.
11. Thierry AR, Mouliere F, El Messaoudi S, Mollevi C, Lopez-Crapez E, Rolet F, et al. Clinical validation of the detection of KRAS and BRAF mutations from circulating tumor DNA. Nat Med 2014;20:430–5.
12. Murtaza M, Dawson SJ, Tsui DW, Gale D, Forshew T, Piskorz AM, et al. Non-invasive analysis of acquired resistance to cancer therapy by sequencing of plasma DNA. Nature 2013;497:108–12.
13. Wan JC, Massie C, Garcia-Corbacho J, Mouliere F, Brenton JD, Caldas C, et al. Liquid biopsies come of age: towards implementation of circulating tumour DNA. Nat Rev Cancer 2017;17:223–38.
14. Maier J, Lange T, Kerle I, Specht K, Bruegel M, Wickenhauser C, et al. Detection of mutant free circulating tumor DNA in the plasma of patients with gastrointestinal stromal tumor harboring activating mutations of CKIT and PDGFRA. Clin Cancer Res 2013;19:4854–67.
15. Xu H, Chen L, Shao Y, Zhu D, Zhi X, Zhang Q, et al. Clinical application of circulating tumor DNA in the genetic analysis of patients with advanced GIST. Mol Cancer Ther 2018;17:290–6.
16. Wada N, Kurokawa Y, Takahashi T, Hamakawa T, Hirota S, Naka T, et al. Detecting secondary C-KIT mutations in the peripheral blood of patients with imatinib-resistant gastrointestinal stromal tumor. Oncology 2016;90:112–7.
17. Joensuu H. Risk stratification of patients diagnosed with gastrointestinal stromal tumor. Hum Pathol 2008;39:1411–9.
18. Revheim ME, Kristian A, Malinen E, Bruland OS, Berner JM, Holm R, et al. Intermittent and continuous imatinib in a human GIST xenograft model carrying KIT exon 17 resistance mutation D816H. Acta Oncol 2013;52:776–82.
19. Namlos HM, Zaikova O, Bjerkehagen B, Vodak D, Hovig E, Myklebost O, et al. Use of liquid biopsies to monitor disease progression in a sarcoma patient: a case report. BMC Cancer 2017;17:29.
20. Kresse SH, Namlos HM, Lorenz S, Berner JM, Myklebost O, Bjerkehagen B, et al. Evaluation of commercial DNA and RNA extraction methods for high-throughput sequencing of FFPE samples. PLoS One 2018;13:e0197456.
21. Langmead B, Salzberg SL. Fast gapped-read alignment with Bowtie 2. Nat Meth 2012;9:357–9.
22. Garrison E, Marth G. Haplotype-based variant detection from short-read sequencing 2012:1–8. arXiv:12073907v2 [q-bioGN].
23. Wilm A, Aw PP, Bertrand D, Yeo GH, Ong SH, Wong CH, et al. LoFreq: a sequence-quality aware, ultra-sensitive variant caller for uncovering cell-population heterogeneity from high-throughput sequencing datasets. Nucleic Acids Res 2012;40:11189–201.
24. Lasota J, Dansonka-Mieszkowska A, Sobin LH, Miettinen M. A great majority of GISTs with PDGFRA mutations represent gastric tumors of low or no malignant potential. Lab Invest 2004;84:874–83.
25. Wardelmann E, Losen I, Hans V, Neidt I, Speidel N, Bierhoff E, et al. Deletion of Trp-557 and Lys-558 in the juxtamembrane domain of the c-kit protooncogene is associated with metastatic behavior of gastrointestinal stromal tumors. Int J Cancer 2003;106:887–95.

Published OnlineFirst August 10, 2018; DOI: 10.1158/1535-7163.MCT-18-0174

26. Martin J, Poveda A, Llombart-Bosch A, Ramos R, Lopez-Guerrero JA, Garcia del Muro J, et al. Deletions affecting codons 557-558 of the c-KIT gene indicate a poor prognosis in patients with completely resected gastrointestinal stromal tumors: a study by the Spanish Group for Sarcoma Research (GEIS). J Clin Oncol 2005;23:6190–8.
27. Singer S, Rubin BP, Lux ML, Chen CJ, Demetri GD, Fletcher CD, et al. Prognostic value of KIT mutation type, mitotic activity, and histologic subtype in gastrointestinal stromal tumors. J Clin Oncol 2002;20: 3898–905.
28. Bettegowda C, Sausen M, Leary RJ, Kinde I, Wang Y, Agrawal N, et al. Detection of circulating tumor DNA in early- and late-stage human malignancies. Sci Transl Med 2014;6:224ra24.
29. Spindler KL, Pallisgaard N, Vogelius I, Jakobsen A. Quantitative cell-free DNA,KRAS, and BRAF mutations in plasma from patients with metastatic colorectal cancer during treatment with Cetuximab and Irinotecan. Clin Cancer Res 2012;18:1177–85.
30. Diehl F, Li M, Dressman D, He Y, Shen D, Szabo S, et al. Detection and quantification of mutations in the plasma of patients with colorectal tumors. Proc Natl Acad Sci U S A 2005;102:16368–73.
31. Taly V, Pekin D, Benhaim L, Kotsopoulos SK, Le Corre D, Li X, et al. Multiplex picodroplet digital PCR to detect KRAS mutations in circulating DNA from the plasma of colorectal cancer patients. Clin Chem 2013;59: 1722–31.
32. Leary RJ, Sausen M, Kinde I, Papadopoulos N, Carpten JD, Craig D, et al. Detection of chromosomal alterations in the circulation of cancer patients with whole-genome sequencing. Sci Transl Med 2012;4:162ra54.
33. Perakis S, Auer M, Belic J, Heitzer E. Chapter three: advances in circulating tumor DNA analysis. In: Makowski GS, editor. Advances in clinical chemistry. Vol. 80. Burlington: Academic Press; 2017. p.73–153.
34. Heitzer E, Ulz P, Geigl JB. Circulating tumor DNA as a liquid biopsy for cancer. Clin Chem 2015;61:112–23.
35. Heinrich MC, Corless CL, Blanke CD, Demetri GD, Joensuu H, Roberts PJ, et al. Molecular correlates of imatinib resistance in gastrointestinal stromal tumors. J Clin Oncol 2006;24:4764–74.
36. Wardelmann E, Thomas N, Merkelbach-Bruse S, Pauls K, Speidel N, Büttner R, et al. Acquired resistance to imatinib in gastrointestinal stromal tumours caused by multiple KIT mutations. Lancet Oncol 2005;6:249–51.
37. Corless CL, Barnett CM, Heinrich MC. Gastrointestinal stromal tumours: origin and molecular oncology. Nat Rev Cancer 2011;11:865–78.
38. Heinrich MC, Maki RG, Corless CL, Antonescu CR, Harlow A, Griffith D, et al. Primary and secondary kinase genotypes correlate with the biological and clinical activity of sunitinib in imatinib-resistant gastrointestinal stromal tumor. J Clin Oncol 2008;26: 5352–9.
39. Garner AP, Gozgit JM, Anjum R, Vodala S, Schrock A, Zhou T, et al. Ponatinib inhibits polyclonal drug-resistant KIT oncoproteins and shows therapeutic potential in heavily pretreated gastrointestinal stromal tumor (GIST) patients. Clin Cancer Res 2014;20:5745–55.
40. Prenen H, Cools J, Mentens N, Folens C, Sciot R, Schöffski P, et al. Efficacy of the kinase inhibitor SU11248 against gastrointestinal stromal tumor mutants refractory to imatinib mesylate. Clin Cancer Res 2006;12:2622–7.
41. Carter TA, Wodicka LM, Shah NP, Velasco AM, Fabian MA, Treiber DK, et al. Inhibition of drug-resistant mutants of ABL, KIT, and EGF receptor kinases. Proc Natl Acad Sci U S A 2005;102:11011–6.
42. George S, Wang Q, Heinrich MC, Corless CL, Zhu M, Butrynski JE, et al. Efficacy and safety of regorafenib in patients with metastatic and/or unresectable GI stromal tumor after failure of imatinib and sunitinib: a multicenter phase II trial. J Clin Oncol 2012;30:2401–7.
43. Hou H, Yang X, Zhang J, Zhang Z, Xu X, Zhang X, et al. Discovery of targetable genetic alterations in advanced non-small cell lung cancer using a next-generation sequencing-based circulating tumor DNA assay. Sci Rep 2017;7:14605.
44. Misale S, Arena S, Lamba S, Siravegna G, Lallo A, Hobor S, et al. Blockade of EGFR and MEK intercepts heterogeneous mechanisms of acquired resistance to anti-EGFR therapies in colorectal cancer. Sci Transl Med 2014;6:224ra26.

Published OnlineFirst August 10, 2018; DOI: 10.1158/1535-7163.MCT-18-0174

Molecular Cancer Therapeutics

Noninvasive Detection of ctDNA Reveals Intratumor Heterogeneity and Is Associated with Tumor Burden in Gastrointestinal Stromal Tumor

Heidi M. Namløs, Kjetil Boye, Skyler J. Mishkin, et al.

Mol Cancer Ther 2018;17:2473-2480. Published OnlineFirst August 10, 2018.